

# UPDATE OF THE ESA METEOROID MODEL

Valeri Dikarev<sup>\*1</sup>, Eberhard Grün<sup>1</sup>, Markus Landgraf<sup>2</sup>, and Rüdiger Jehn<sup>2</sup>

<sup>1</sup>Max-Planck-Institut für Kernphysik, Heidelberg, Germany

<sup>2</sup>ESA/ESOC, Darmstadt, Germany

## ABSTRACT

The ESA meteoroid model was recently updated to fix errors in the computer code reported by its user community. This opportunity was taken for an extended revision, the orbital distributions of meteoroids were also improved. Their resolution was enhanced substantially, the definition of the meteoroid populations was modified to allow for higher flexibility and therefore better fit to observations. The infrared sky maps from COBE, Galileo's dust detector data from the interplanetary cruise, Ulysses dust detector data up to the end of 2003, and the microcrater counts on the lunar rocks retrieved by the Apollo missions are the basis for the model update. The model successfully passes the tests against those data not incorporated, namely the spin-averaged fluxes on the Helios 1 dust detectors, the first four years of the Pioneer 11 impact records as well as radar meteor observations. The orbital evolution of meteoroids taken into account in the ESA model allows for more reliable extrapolations beyond the incorporated data than the previous empirical models could provide.

Key words: Interplanetary medium, Meteoroid model.

## 1. INTRODUCTION

Delivered in 2003 to ESOC, the new ESA meteoroid model was planned for incorporation in the MASTER model of orbital debris by the Technical University of Braunschweig in Summer 2004. It was soon realised, however, that the flux prediction software, albeit tremendously faster than its predecessors (at the same accuracy), is too slow to call from the end user-oriented MASTER programme. Several ways to accelerate the meteoroid model predictions for the MASTER were investigated, including the development of a driver subroutine to be compiled and executed inside the MASTER process rather than

launching an external program. The new driver subroutine presented a completely new and independent interface to the meteoroid populations, allowing for tests of the meteoroid model software that had been impossible before. These tests did reveal errors in the meteoroid model software eventually, and these errors were corrected in 2004. The corrected version of the software was delivered to ESOC. The meteoroid model was re-adjusted as well to the observations using the correct software.

As the correction and re-adjustment were time-consuming, it was decided to take the opportunity for an extended revision of the model, including the resolution enhancement in orbital space, and removal of some of the a-priori constraints. The constraints on the populations in the 2003 release impacted the flexibility of model fit to observations.

More data were incorporated on this opportunity as well. In addition to the interplanetary meteoroid flux (Grün et al. 1985), the Cosmic Infrared Background Experiment (COBE) satellite-produced sky maps through the 4.9, 12, 25 and 60  $\mu\text{m}$ -wavelength filters, another map was used, the one obtained through the 100  $\mu\text{m}$  filter. The most recent data from Ulysses were taken up to the end of 2003, while the original model was based on the data up to the end of 1999 only. The Galileo data were used as before, yet the spin-angle information was taken into account whenever possible.

It is necessary to note that all these corrections were done before the model was first described in paper (Dikarev et al. 2005a,b), except the final report of 2003 that has been available from ESOC, and a few conference abstracts. However, the user community must be warned against application of any version of the meteoroid model, including its software, that could have been distributed before 2004.

After the errors were corrected and the new model parameters were inferred, the model was for the first time additionally tested against those data not incorporated. The Pioneer 11 and Helios 1 impact records were not used to adjust the model parameters because of their statistical insignificance with respect to the rich data sets from the Ulysses and

<sup>\*</sup>On leave from Astronomical Institute of St. Petersburg University, Russia.

Galileo spacecraft, as well as some uncertainties in modelling the dust detectors on board Pioneer and Helios. However, the early deep space mission data are now used to test the model.

## 2. AN UPDATE OF COMPUTER CODE AND METEOROID MODEL

A computer code to estimate the number density, flux and average impact speed (hereafter, the observables) of meteoroids on a target in the Solar system and near Earth was described in (Dikarev et al. 2005a). It is capable to read meteoroid populations of the old models (Divine 1993; Staubach et al. 1997) that were composed of the distributions separable in perihelion distance, eccentricity and inclination. It supports a new format as well of the three-dimensional distributions in orbital elements that are the only way to describe a physically realistic meteoroid cloud. The code can calculate the observables along an arbitrary spacecraft trajectory defined in terms of the orbital elements or Cartesian coordinates and velocities, in a variety of reference frames, with the primary body being either the Sun or Earth. In the vicinity of Earth, the code takes the gravitational focusing of meteoroids into account, in accord with the formalism developed by Divine (see Staubach et al. 1997). When calculating the flux of meteoroids, the exposed area can be an arbitrary function of the incidence angle measured from the symmetry axis.

In the recent (2004) update of the code some minor errors were corrected that were never hit in the course of model fit to data, and one typographical mistake was fixed in the number density calculations. Although number density predictions are not the primary goal of the model, they are necessary to fit the model to one of the key data sets, i.e. the infrared sky maps due to the Cosmic Background Explorer (COBE) satellite. Discovery of this mistake in the code necessitated a new fit of the meteoroid model to the COBE data as well as to the other data sets incorporated before.

The computer code for meteoroid models is best suited to derive the observables for large clouds of meteoroids, e.g. from all comets or from all asteroids. Thin clouds due to specific sources occupying small volumes in the orbital space require higher orders of the quadratures to estimate the integrals involved accurately. Therefore, it takes much longer to calculate the observables for all meteoroid populations when fitting the population weights than to calculate the flux on spacecraft when the model is already consolidated. For  $\sim 10^5$  incorporated measurements, most of them being the line-of-sight brightness integrals corresponding to the COBE observations, and for 79 populations of interplanetary and interstellar dust, the preparation work to solve the inverse problem takes weeks on a desktop computer.

Given the long duration of the re-adjustment works,

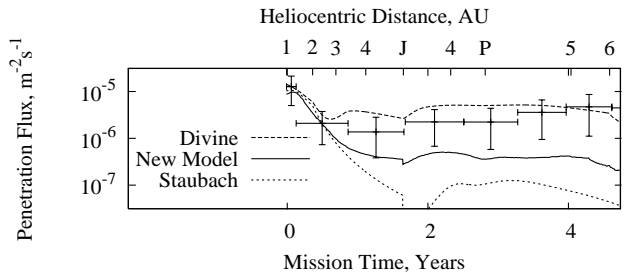


Figure 1. Fluxes inferred from the Pioneer 11 impact counts, taking the uncertainty of the number of active cells of dust detector into account (Dikarev & Grün 2002) shown with error bars, and the meteoroid model expectations plotted as curves. On the heliocentric distance axis, ‘J’ marks the Jupiter fly-by, and ‘P’ marks the perihelion of the post-Jupiter orbit.

the decision was made to update the model on this opportunity as well. In particular, its resolution in the orbital space was enhanced. The eccentricity dimension of the 3-D array of the orbital distributions was expanded from 20 to 100. This was done to resolve the low-eccentricity orbits of dust particles from asteroids that are gradually circularised by the Poynting-Robertson effect and by the time of crossing the Earth orbit they all clumped in one or two eccentricity bins in the previous model. The inclination dimension was kept at 180 (one bin spans over one degree). The perihelion distance dimension was kept at 50 (with the bins spaced logarithmically), however, the range of the element was reduced from 18 AU to 6 AU, reflecting the fact that in the present model there are no sources nor dynamics capable to insert meteoroid particles at perihelia  $\geq 5.7$  AU.

The population generation software was updated as well to meet the requirements of the new resolution. In the first model release, we bound some population weights according to their sources. For example, the dust particles from comets in the region of close encounters with Jupiter must have had the same phase density with the particles leaking from the region under the Poynting-Robertson effect, at the inner boundary of the region. This constraint based on continuity considerations was not confirmed by our more recent numerical simulations, reflecting a more complicated topology of the leaking trajectories than in our first simplistic assumption. These constraints were therefore removed to let the fit to observations resolve the uncertainty.

## 3. NEW TESTS OF THE METEOROID MODELS AGAINST INDEPENDENT DATA

New comparisons of the meteoroid model predictions were made with those data sets not incorporated. They show unambiguously the strength of the physical approach adopted in the new model. Incorporation of the orbital evolution of meteoroids leads

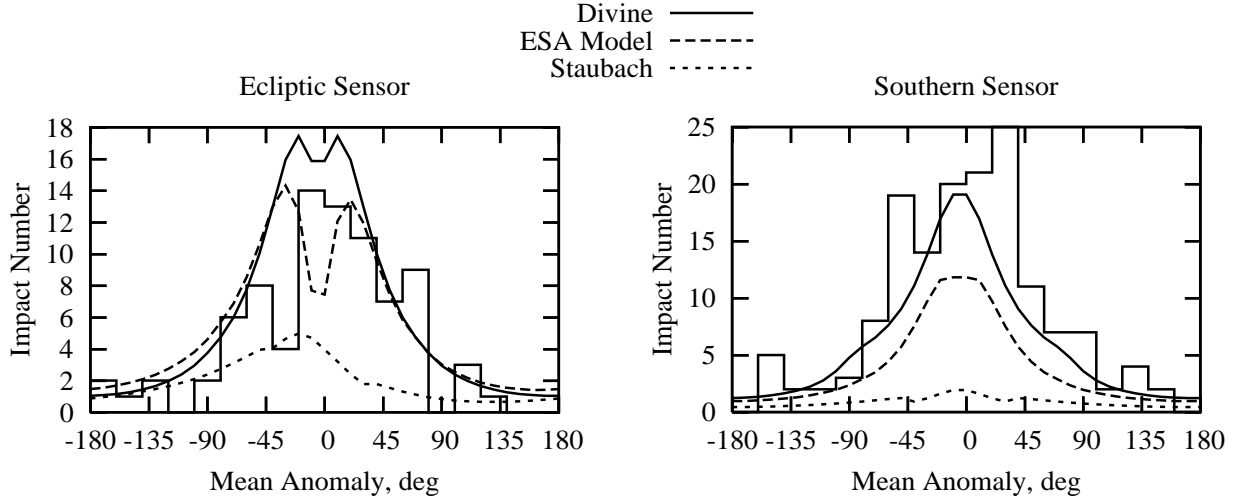


Figure 2. Impact counts with the dust detectors on board Helios 1 (step-functions) and their theoretical counterparts calculated with the Divine, Staubach, and the new model.

indeed to a great improvement of the quality of extrapolations. The empirical models by Divine and Staubach are good short descriptions of those data sets incorporated, however, every new data set would most likely require their re-formulation.

The Pioneer 11 spacecraft carried a dust detector into the outer Solar system (Humes 1980). It was composed of cans filled with gas protected from space by thin foil only. When the foil was punctured by a meteoroid, a drop of the gas pressure was detected and recorded as an impact event. The event meant the end of the can. Although it was not known which can was punctured, the entire set of cans was divided into two sub-sets with independent electronics for redundancy. Both sub-sets reported impacts, however, the ratio of the numbers of impacts was unbelievably different from the ratio of the numbers of cans in the sub-sets, despite very similar fields of view of the sub-sets. A partial damage of the cans at launch was proposed to resolve the difference (Dikarev & Grün 2002), and based on a probabilistic model of the dust instrument exploiting its built-in redundancy, the true fluxes as well as the confidence intervals were re-derived from the raw data.

The true fluxes and the confidence intervals are shown in Fig. 1 along with the predictions by the Divine, Staubach, and the new models. All the models are in agreement with the data during the first year of the mission, i.e. before the spacecraft has left the region where each model has been based on many data sets. The Pioneer data were in the foundation of the Divine model, and it works very well up to 6 AU from the Sun where we stop our test. The data set was not incorporated in the Staubach model, and its predictions go far away from the confidence intervals. In contrast, the new model diverges from measurements significantly less than the Staubach model, in spite of the fact that the data set was not incorporated either. Note that the Divine model explained

the Pioneer 11 data with the help of the so-called “halo” population (see below our comparison with the Ulysses data set, however).

The Helios 1 spacecraft was sent to an elliptic orbit in the ecliptic plane with the perihelion distance of 0.3 AU and the aphelion distance of 1 AU. It was equipped with two low-area dust detectors capable to perform chemical analysis of the impactor material. One of the detectors was mounted to look into the ecliptic plane, and the other was looking toward the southern hemisphere. They both spun along with the spacecraft about the axis perpendicular to the ecliptic plane. The low target area of these detectors enabled the instruments to obtain mass-spectra, however, it permitted to detect a relatively small number of impacts only, in spite of a long exposure time (5 years).

For each impact, the ion charge of the released plasma cloud was measured and categorized in four ranges of magnitude. We excluded the lower range 1 and estimated the numbers of impacts in ranges 2 through 4 using the Divine, Staubach and the new models (see Fig. 2). The Helios 1 data were in the base of the Divine model, and the model is in a good agreement with the data. Simultaneously, the new model performs considerably good on the data set, despite it was not incorporated. The Staubach model was not based on the Helios data and can not be used to predict meteoroid fluxes close to the Sun, although it is close to the measurements when the spacecraft is in the aphelion of its orbit, i.e. at the Earth’s heliocentric distance where many data sets constrain all models.

The Ulysses data were incorporated in the Divine model in a very preliminary version only, for the spacecraft had just begun its cruise to Jupiter. No information on spin angles was used from the experiment results. In contrast, the Staubach and the new

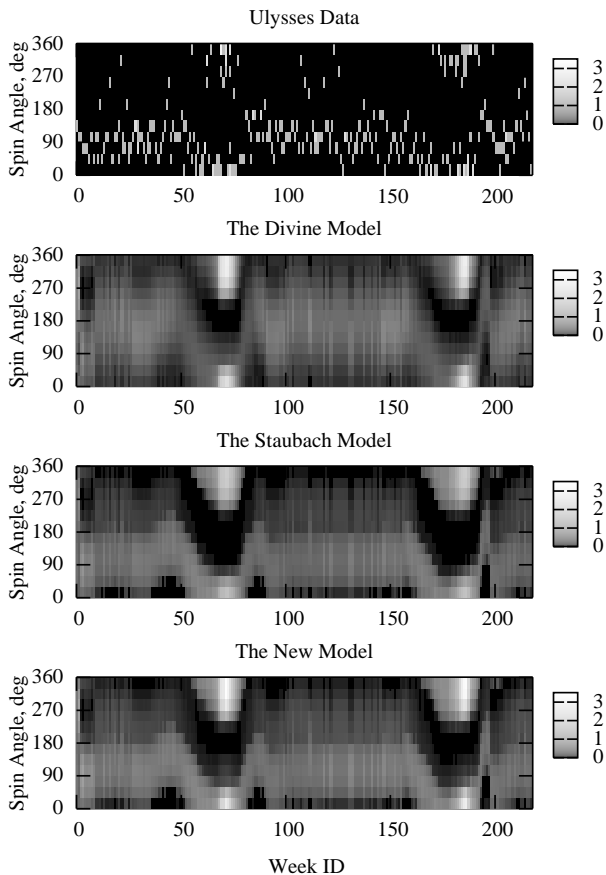


Figure 3. Impact counts reported by the Ulysses dust detector, for those weeks when at least one impact was detected, and their theoretical counterparts. The gray levels indicate the impact numbers.

models are based on the Ulysses data extensively. The directionality of impacts into the Ulysses dust detector helped to discover and explore the interstellar dust flux through the Solar system.

Figure 3 compares the time and spacecraft spin angle distributions of impacts into the Ulysses dust detector in the data and predicted by the three meteoroid models. The Staubach and the new model perform good on this data set that was incorporated in each of them. However, the Divine model predicts a substantially different distribution of spin angles of the impacts. In fact, the Ulysses data rejects the “halo” population introduced by Divine to explain the Pioneer 11 data (see above). The “halo” population is dominant in the Divine model plot away from the ecliptic plane and is missing from the data map. The ecliptic plane crossings near the perihelion of the Ulysses’ orbit took place near week numbers 60 and 180. At these times, high rates were detected and predicted by all models around zero spin angle. The flux was due to the dust near the ecliptic plane. Since the inclination of the spacecraft orbit was high, it flew from the ecliptic south to north very fast relative to this dust, while the spin angle is measured from the ecliptic north. The Divine model predicts a dust cloud more confined to the ecliptic plane than

the Staubach and the new model: the flux enhancements last longer.

Obviously, the new model benefits from the physical approach to construction of meteoroid populations, i.e. taking the orbital evolution of the particles into account. Its extrapolations beyond the observational base are more reliable than those of the previous models that are only good to describe those data sets incorporated.

#### 4. METEOROID RADIANT MAPS FOR SOLAR SYSTEM PLANETS

We have also built the maps of meteoroid radiants for the Earth and Mercury, based on the Divine, Staubach, and the new model. The Earth map is interesting to compare with the results of radio meteor surveys, while the Mercury map construction was inspired by one of the future ESA missions, Bepi-Colombo. The maps do not take the gravitational focusing into account, so they are only applicable to spacecraft on distant, low-velocity orbits about the corresponding planet.

Figure 4 shows the radiant maps for the Earth. The fluxes of particles greater than  $10^{-3}$  g in mass (collisional dynamics in the new model, the meteoroids are destroyed before they leave the parent body orbit) are shown on the left-column maps, as seen through a circular field of view of ten-degree radius. The fluxes of particles greater than  $10^{-9}$  g in mass (Poynting-Robertson dynamics in the new model, the dust spirals toward the Sun) are on the right-column maps.

Despite the Harvard Radio Meteor Project (HRMP) data were incorporated in the Divine model, shaping its “core” and “asteroidal” populations that were left intact in the Staubach model, the models do not show the most prominent features of the meteor surveys, i.e. the “Helion” ( $180^\circ$  solar longitude in the ecliptic plane), “Anti-Helion” ( $0/360^\circ$ ), and the “Apex” ( $90^\circ$ ) meteor rate enhancements (Taylor & Elford 1998, their Fig. 4). In contrast, the new model reveals all of them, despite the radar data were not incorporated.

However, the “Apex” source is not resolved into the northern and southern rate sub-enhancements. The “Helion”, “Anti-Helion” and “Apex” enhancements are better seen in the map for big particles that the HRMP radar was more sensitive to. The enhancements near the poles above and below the apex, the “South” and “North Toroidal”, are rather strong in the new model’s map for small dust grains. They are due to the dust from asteroids that spirals toward the Sun under the Poynting-Robertson effect.

The radar data on meteors are notoriously difficult to correct for all biases. Several modifications of the correction method were proposed recently (Taylor & Elford 1998; Galligan & Baggaley 2004). Therefore, we attempted to simulate the effect of an un-

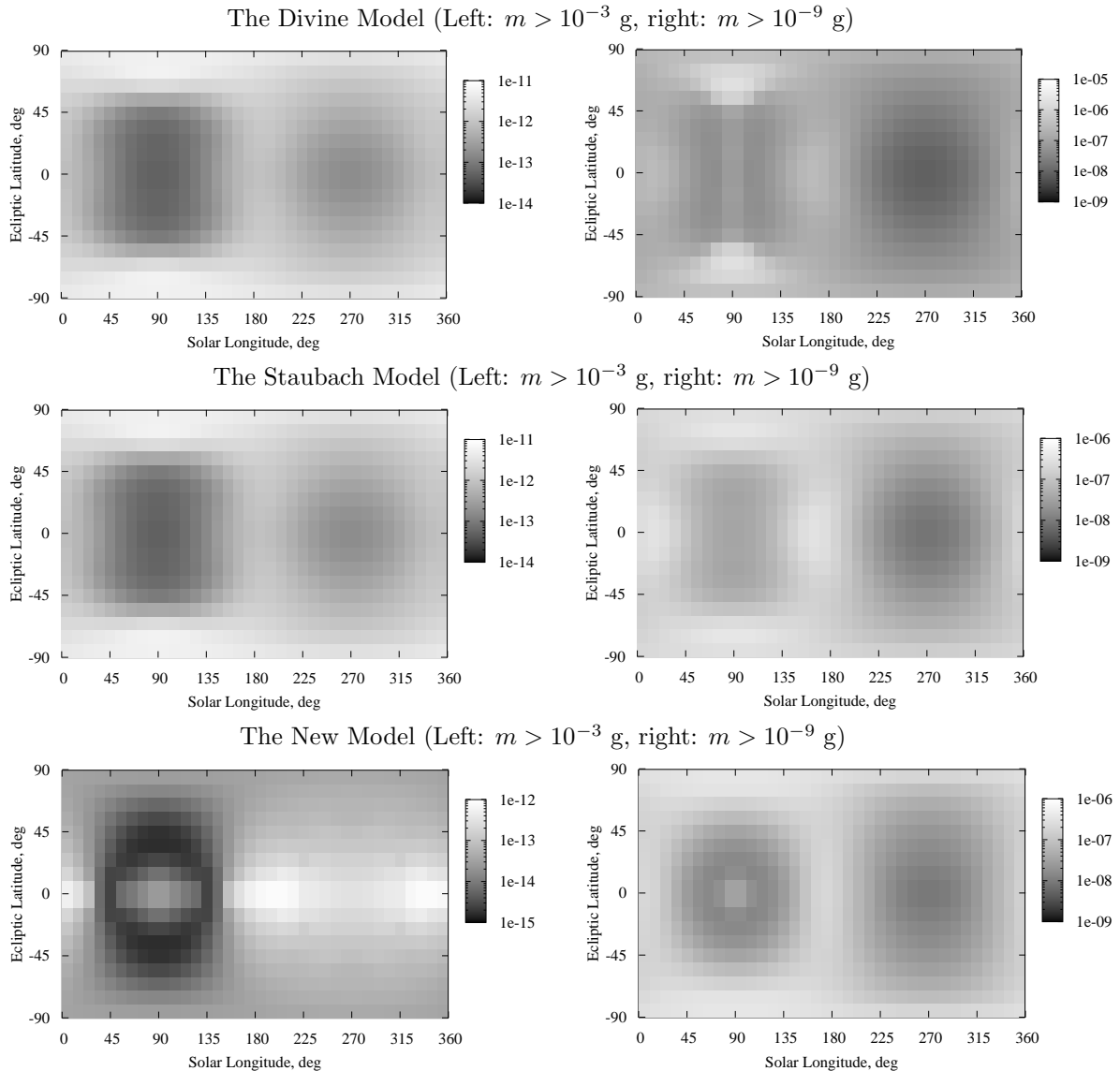


Figure 4. Meteoroid radiant map at the Earth. Shown are the fluxes, per square metre per second, through a circular field of view of ten-degree radius. The solar longitude is measured from the anti-solar direction in the ecliptic plane counterclockwise, so that the apex of the Earth is at  $90^\circ$ .

accounted bias depending on meteor velocity when building the radiant maps at the Earth. We found that even a linear additional correction for velocity changes the ratios of the rate enhancements substantially, revealing the “Apex” source and darkening the broad background around the antapex direction.

Figure 5 is devoted to Mercury. The new meteoroid model reveals more differences in meteoroid radiants between Earth and another location in the Solar system. In the previous models, the assumption of mathematical separability of the orbital distributions did not allow the orbits to circularise under the Poynting-Robertson drag with the decrease of the semimajor axis. The circularisation reduces the tangential component of the meteoroid velocity relative to a planet on a circular orbit, and therefore the radiants of the small dust grains ( $> 10^{-9}$  g) ap-

pear to avoid the apex and antapex directions due to the dominant radial and normal components. The effect is opposite for the big particles ( $> 10^{-3}$  g) because the eccentricities of the big meteoroids able to reach Mercury from Jupiter-crossing orbits have to be higher than of those able to reach the Earth.

## 5. SUMMARY

We report an update of the ESA meteoroid model after a fix pack was applied to the computer code used to predict the observations. In the new code and model, the resolution of the meteoroid population distributions in orbital elements is enhanced, the unnecessary constraints on the populations are removed to allow for a higher flexibility of model fit

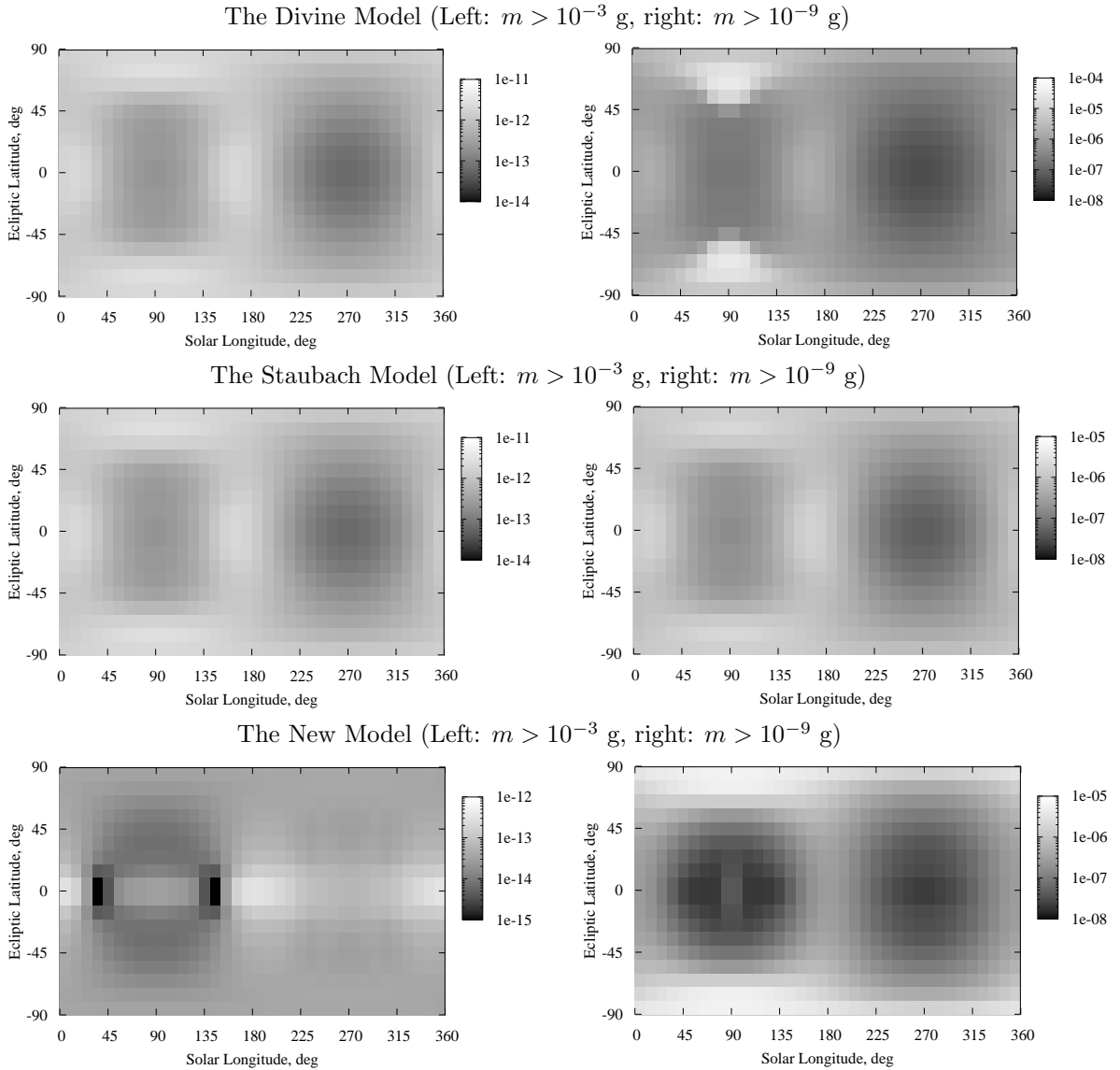


Figure 5. Meteoroid radiant map at Mercury. See the previous figure for explanations.

to observations.

More comparisons are reported of the ESA meteoroid model as well as the earlier models by Divine (1993) and Staubach et al. (1997) with the measurements by the dust detectors on board Pioneer 11 and Helios 1. It is shown that the new ESA model incorporating the orbital evolution of meteoroids is more reliable when extrapolating the available observations, while the previous models disagree with the data sets that had not been included.

## 6. ACKNOWLEDGEMENTS

The authors are grateful to Mr. Stabroth of the Tech. Univ. of Braunschweig for his indispensable contribution to testing the meteoroid model software.

## REFERENCES

- Dikarev V., Grün E., Jan. 2002, *Astron. Astrophys.*, 383, 302
- Dikarev V., Grün E., Baggaley J., et al., 2005a, *Adv. Space Res.*, in press
- Dikarev V., Grün E., Baggaley J., et al., 2005b, *Earth Moon Planets*, submitted
- Divine N., 1993, *J. Geophys. Res.*, 98, 17029
- Galligan D.P., Baggaley W.J., Sep. 2004, *Mon. Not. R. Astron. Soc.*, 353, 422
- Grün E., Zook H.A., Fechtig H., Giese R.H., 1985, *Icarus*, 62, 244
- Humes D.H., Nov. 1980, *J. Geophys. Res.*, 85, 5841
- Staubach P., Grün E., Jehn R., May 1997, *Adv. Space Res.*, 19, 301
- Taylor A.D., Elford W.G., Jun. 1998, *Earth Planets Space*, 50, 569